ISSN No: -2456 –2165

Evolution and Comparision on CFD Simulation of Phase Change Materials (PCMS) in a Spherical Capsule

M.Senthil Kumar*, T.Parameswaran Pillai**
*M.E Energy Engineering Student
** Asst. Prof of Anna University, Trichy Campus

Abstract:-The present study is focused on CFD simulation of constrained melting of Phase Change Materials (PCMs) in a spherical container. To investigate the melting process of the PCM, its melting fraction was analyzed at different times. The results indicated the existence of thermally stable layers on the top of the sphere. Moreover, inspection of the calculated temperatures at different points along the vertical axis indicates the existence of some disturbances at the bottom of the sphere due to the natural convection. After the validation of the results, the effects of different parameters such as the surface temperature of the capsule, the initial temperature and the size of the spherical capsules, on the melting process were investigated. The initial temperature did not affect the melting rate, whereas melting rate increased by increasing the surface temperature of the capsule and also decreasing the diameter of the sphere. The results showed that the surface temperature of capsule compared to geometrical parameters and other operational conditions can have a greater influence on the melting rate and the heat flux. Comparing with different materials to estimate the characteristics of phase change materials.

Keywords: Phase Change Material, SAT, Paraffin Wax, Characteristics of PCMs.

I. INTRODUCTION

Recently, latent heat thermal energy storage systems have been widely applied in cool storage for central air-conditioning, hot storage for air heating, solar energy, energy efficient buildings and waste heat recovery. Storage systems allow for the efficient and rational utilization of the available resources or renewable energies, by using the time lag between production, as well as the availability of the energy and its consumption in the demanding systems. Phase change materials (PCM) are mainly used to provide higher storage densities. As a serious problem PCMs have relatively low thermal conductivities. Therefore, increasing the surface/volume ratio of PCMs in order to increase the heat-transfer rate is very appealing. This can be done by packing a volume with a great number of PCM capsules. The spherical geometry is one interesting case for heat storage applications, since spheres are much employed in packed beds. Due to the complexity of such systems, it is often more effective to first model the behavior of an individual sphere and then describe it with a simple parametric model in the packed bed modeling. Roy and Sengupta (1989) examined the melting process with the solid phase initially uniformly super cooled. In order to include the effects of a temperature gradient in the solid core, they modified the heat transfer equation. At each time step, the unsteady conduction equation has been solved numerically using a toroidal coordinate system with a suitable immobilization of the moving boundary to transform the infinite domain into a finite one. In another paper (Roy and Sengupta, 1990), they investigated the outcome of natural convection on the melting process. In order to reduce the computational effort and the time, they made some simplifications. They obtained the non-dimensional melting time and the heat transfer coefficient as functions of the PCM property values, the operating temperature and the physical size. Ettouney et al. (2005) experimentally evaluated the heat transfer (during energy storage) and release for the phase change of paraffin wax in the spherical shells. They showed that an increment in the Nusselt number of the sphere with a larger diameter is attributed to the increase in the natural convection cells in the PCM inside the sphere.The natural convection role is enhanced upon an increase in the sphere diameter and the air temperature. On the other hand, during solidification the wax layers are formed inward, nucleating on the sphere walls. As solidification progresses, the melt volume becomes smaller and the role of natural convection diminishes rapidly. Khodadadi and Zhang (2001) also considered the effects of buoyancy-driven convection on the constrained melting of phase change materials within spherical containers. They reported that during the initial melting process, the conduction mode of the heat transfer is dominant. As the buoyancy driven convection is strengthened due to the increase in the melting zone, the process at top region of the sphere is much faster than at the bottom due to the increment of the conduction mode of heat transfer. They found that buoyancy driven convection speeds up the melting process compared to the diffusion-controlled melting. Assis et al. (2007) numerically and

experimentally explored the melting process of a PCM in a spherical geometry. The results of their experimental investigation, including visualization, were favorably comparable with the numerical results and therefore suitable for validation of the mathematical approach. Their computational results showed how the transient phase-change process depends on the thermal and geometrical parameters of the arrangement. Veerappan et al. (2009) investigated the phase change behavior of 65 mol% capric acid and 35 mol% lauric acid, calcium chloride hexa hydrate, *n*-octadecane, *n*-hexadecane, and *n*-eicosane inside the spherical containers to identify a suitable heat storage material. They created analytical models for solidification and melting of PCM in a spherical shell with conduction, natural convection, and heat generation and found a good agreement between the analytical predictions and the experimental data. Both models were validated with the experimental work of Eames and Adref (2002). Regin et al. (2006) examined the heat transfer performance of a spherical capsule using paraffin wax as PCM placed in a convective environment during the melting process. The model results were in a good agreement with the experimental data. Tan (2008) investigated the melting of the phase change material (PCM) inside a sphere using n-octadecane for both constrained and unconstrained melting processes. For constrained melting, paraffin wax (n-octadecane) was immobilized, through the use of thermocouples when melting is done inside a transparent glass sphere. Their experimental setup provided a detailed temperature data that were gathered along the vertical diameter of the sphere during the melting process. Tan et al. (2009) also experimentally and numerically investigated the constrained melting of PCMs inside a spherical capsule to understand the role of the buoyancy-driven convection. In this study, a computational fluid dynamics (CFD) modeling on the constrained melting of phase change material (PCM) in a spherical container was performed. The effects of different parameters like the capsule size, the surface temperature, the initial temperature and the Stefan number, on the PCM melting process were investigated.

II. CFD SIMULATION

CFD simulation was carried out using the commercial Fluent 6.3 software. The physical model and computational procedure are discussed below.

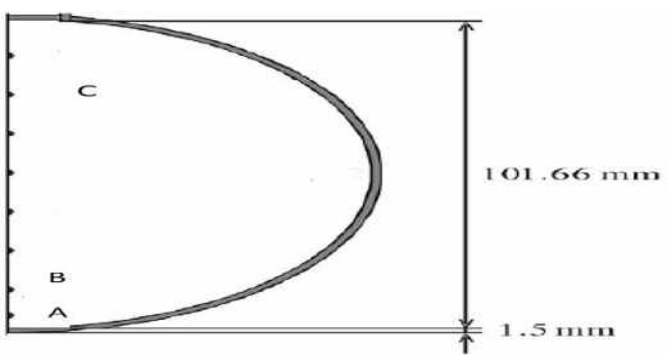

Fig. 1: The Computational Domain.

A. *Physical model*

Consider a spherical shell with an internal radius (Ri) of 50.83 mm and a wall thickness of 1.5 mm initially filled with a solid PCM at an initial temperature (Ti) lower than the melting temperature (Tm). The schematic diagram of the physical model is shown in Fig. 1. At t (time) > 0, a constant temperature (T0) greater than the melting temperature is imposed on the surface of the sphere, i.e .T0 > Tm. Melting starts at the surface, moving the solid–liquid interface toward the middle of the field. Since the present work is focused on the analysis of constrained melting, both the solid and liquid phases have the same density. The container was made of glass with a thermal conductivity of 1.14 Wm−1 K−1. The properties of the PCM, based on n-octa decane as a commercially available material, are given in Table 1. For the experimental data that we used (Tan, 2008), the initial temperature was 1 °C below the melting temperature and the surface temperature was 40 °C. The Prandtl, Stefan and Rayleigh numbers for this problem were 59.6, 0.113, and 2.63 × 108, respectively.

B. *Computational Procedure*

The numerical approach makes it possible to predict specifications of the melting process that take place inside the sphere. The flow was considered unsteady, laminar, incompressible and two-dimensional. In order to simulate the constrained melting, it is supposed that both the liquid and the solid phases are isotropic, homogeneous and remain in thermal equilibrium at the interface. For the phase-change region inside the PCM, enthalpy-porosity approach (Fluent, Inc., 2006; Voller and Prakash, 1987) was used. In this technique, the melt interface is not tracked explicitly. Alternatively, a quantity called the liquid fraction, indicating the fraction of the cell volume that is in liquid form, is associated with each cell in the domain. In this way, the governing equations for the PCM are as follow

Continuity:

$$(\partial \rho / \partial t) + \nabla(\rho.V) = 0 \nabla \partial$$

∂

where V is the fluid velocity vector, ρ is the density, _ is the dynamic viscosity, P is the pressure, g is the gravitational acceleration, k is the thermal conductivity and H is the specific enthalpy, which is defined as the sum of the sensible enthalpy (h) and the latent heat (ΔH):

$$H = h + \Delta H \quad (4)$$

The content of the latent heat can vary between zero (for a solid) and L (for a liquid):

$$\otimes H = \circledR L \quad (6)$$

Melting temperature	28.2 °C
Density	772 kg m−3
Kinematic viscosity	5 × 10−6 m2s−1
Specific heat	2330 Jkg−1 K−1
Thermal conductivity	0.1505Wm−1 K−1
Latent heat of fusion	243.5 kJ kg−1
Thermal expansion coefficient	0.00091 K−1

Table 1 Thermophysical Properties of N-Octadecane

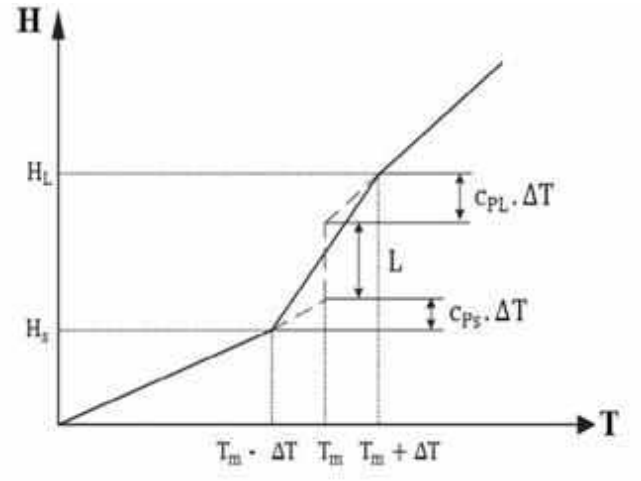

Fig. 2 – The Relation between Enthalpy and Temperature of A Pure Substance

By definition, solidus and liquidus temperatures are the maximum temperature at which the material is at solid state and minimum temperature at which the material is at liquid state, respectively. However, for melting of a pure substance, phase change occurs at a distinct melting temperature. Therefore, solidus and liquidus temperatures are the same. In order to determine the liquid fraction at mushy zone, according to the method was given by Voller and Prakash (1987), a tiny temperature interval, ΔT near the melting point temperature (Tm) was considered and assumed that liquefaction occurs at a certain range of temperature ($Tm - \Delta T$ and $Tm + \Delta T$), as shown in Fig. 2. Consequently, using Equation (7) and by substituting $Tm - \Delta T$ and $Tm + \Delta T$ for *Tsolidus* and *Tliquidus* respectively, liquid fraction was calculated. The source term S in the momentum equation is the Darcy's law damping term that is added to the momentum equation due to the phase change effect on the convection. The coefficient C is a mushy zone constant. This constant measures the amplitude of the damping.The higher this value, the steeper is the transition of the velocity of the material to zero as it solidifies. Values between 104 and 107 are the recommended values for most calculations (Fluent, Inc., 2006) and values exceeding this range may cause the solution to oscillate. In the present research, different values of the constant C were investigated to examine the effect of the mushy zone constant.

In order to handle pressure–velocity coupling, SIMPLE (semiimplicit method for pressure-linked equations) algorithm of Patankar (1980) was employed. The PRESTO scheme was used for the pressure correction equation. This scheme uses the discrete continuity balance for a "staggered" control volume about the face to compute the "staggered" pressure (Patankar, 1980). For flows with natural convection, rotating flows, and flows in strongly curved domain, using PRESTO scheme is recommended (Fluent, Inc., 2006). Other equations (i.e. momentum and energy) were discretized using power law scheme, which interpolates the value of a variable using the exact solution to a one-dimensional convection–diffusion equation.The underrelaxation factors for the velocity components, thermal energy, pressure correction and liquid fraction were 0.1, 0.3, 1 and 0.9, respectively.

Different grid densities were tried to make sure that the solution is independent from the adopted grid density (see Fig. 3). As a result, 7200 grids were found sufficient for the present study. Adopting a fine grid distribution in the radial direction allows for the use of longer time steps. The time required for achieving the full melting is a good measure of time step dependence. By comparing the selected quantities obtained from simulations using 0.05, 0.1, 0.5 and 1 s, the time step for integrating
the time derivatives was set to 1 s.

III. RESULTS AND DISCUSSION

The effect of different values of the mushy zone constant on the melt fraction with a Stefan number of 0.132 and a shell diameter of 101.66 mm, is shown in Fig. 4. As one can see from this figure, the value of 107 is suitable for the present simulation where the numerical result is in most accordance with the experimental data. Fig. 4 also confirms the validation of the result of CFD work. The colored contours of solid–liquid front of the PCM at various time instants for constrained melting process at a wall temperature of 40 °C and an initial temperature of 27.2 °C are shown in Fig. 5.The blue and red colors represent the solid and melted parts, respectively. In the beginning of the process, the outer surface of the solid PCM is in contact with the inner wall of the sphere so that heat conduction dominates between the solid PCM and the wall. This makes the formation of a thin layer of liquid between the solid PCM and the wall of the sphere.

ISSN No: -2456 –2165

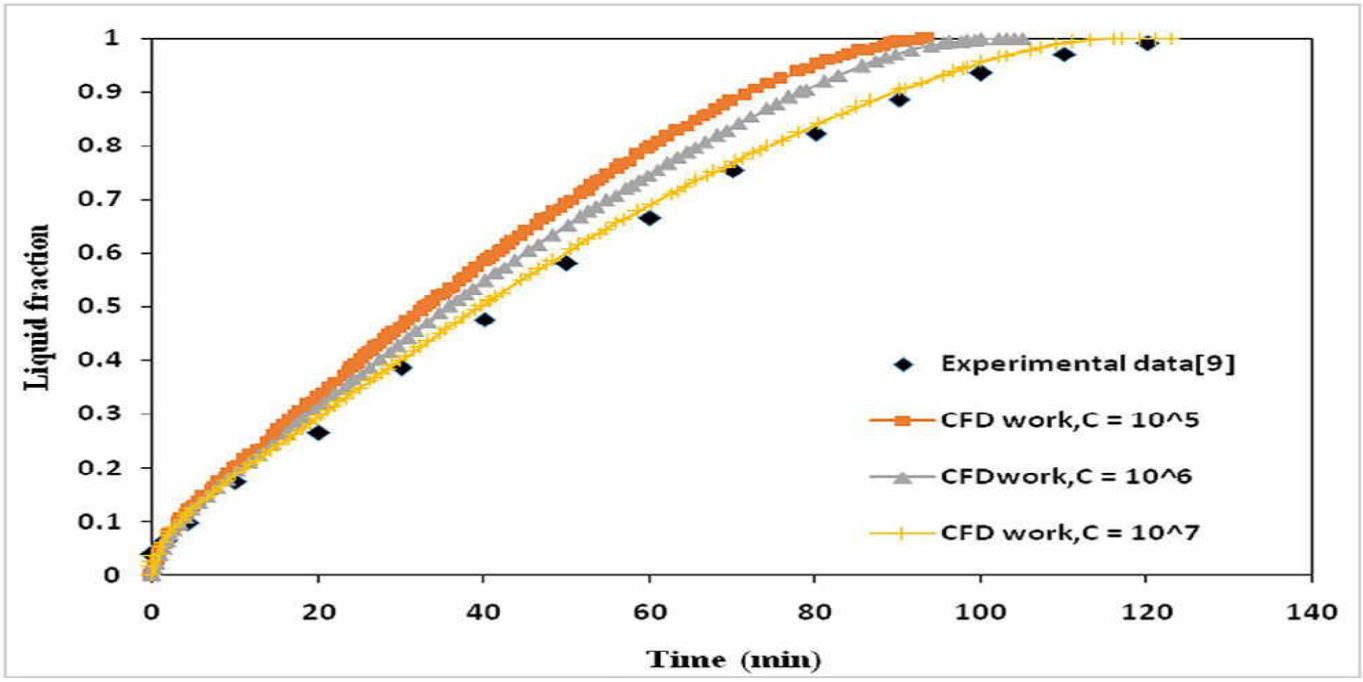

Fig. 4 – Variations in the Liquid Fraction Vs. Time At Different Mushy Zone Constants (Ste = 0.113 And D = 101.66 Mm).

IV. SIMULATION PROCESS PROCEDURE

As time progresses, the molten zone expands and the liquid layer grows. The liquid film is then forced up on the interior surface of the sphere, occupying the region above the solid PCM. By moving toward the top part of the sphere, the warm liquid is replaced with the cold liquid. Therefore, natural convection in combination with a hot rising curved wall jet is dominant at the top and side regions of the sphere. After 40 and 60 minutes, as can be seen in Fig. 5, more intense melting in the upper zone compared to the side and bottom sections is observed. This phenomenon is attributed to the strong role of natural convection in the upper zone of the sphere. After 40, 60 and 80 minutes, a waviness at the bottom part of the PCM is observed. This can be attributed to the existence of stable and unstable thermal layers at the bottom part of the sphere. This result as well as the observed shape of the solid, are in good agreement with the experimental data in the literature (Tan, 2008). The temperature contours of the right side of the sphere as well as the streamlines of the left side of the sphere, at a wall temperature of 40 °C for a sphere of 101.66 mm diameter, are shown in Fig. 6. At 20 and 40 minutes, formation of recirculating vortexes between the solid PCM and the inner wall of the sphere as a result of the replacement of the warm liquid with cold liquid at the bottom part of the sphere is obvious. It can also be seen that more melting occurs at the upper part of the sphere due to the contribution of natural convection (see Fig. 5). The whole PCM is melted after 120 minutes. Comparison of experimental temperatures with the results of CFD simulation for three points A, B, and C along the vertical diameter of the sphere (see Fig. 1) is shown in Fig. 7. The disordered temperature data at points A and B, show the chaotic convection motion in the unstable liquid layer at the bottom of the sphere. The computed temperatures at point C (located on the upper side of the sphere) are in a good agreement with the experimental data. This is due to the stable nature of the liquid layer at the upper part of the sphere. To prove the existence of liquid layer where the point A is located, the variation of liquid fraction at the point A during melting time was calculated (see Fig. 8). The results revealed that the PCM was at a transition state from solid to liquid during 7.5 to 9.5 minutes and after 9.5 minutes it was completely at liquid state.Therefore, the high frequency oscillation in the temperature versus time may be found at this point. The effect of initial temperature is showed in Fig. 9. It is observed that different initial temperatures do not have a substantial effect on the melting process. The melting rates for initial temperatures of 18.2 °C and 8.2 °C are the same but the initial temperature of 27.2 °C has a few faster melting rate.

ISSN No: -2456 –2165

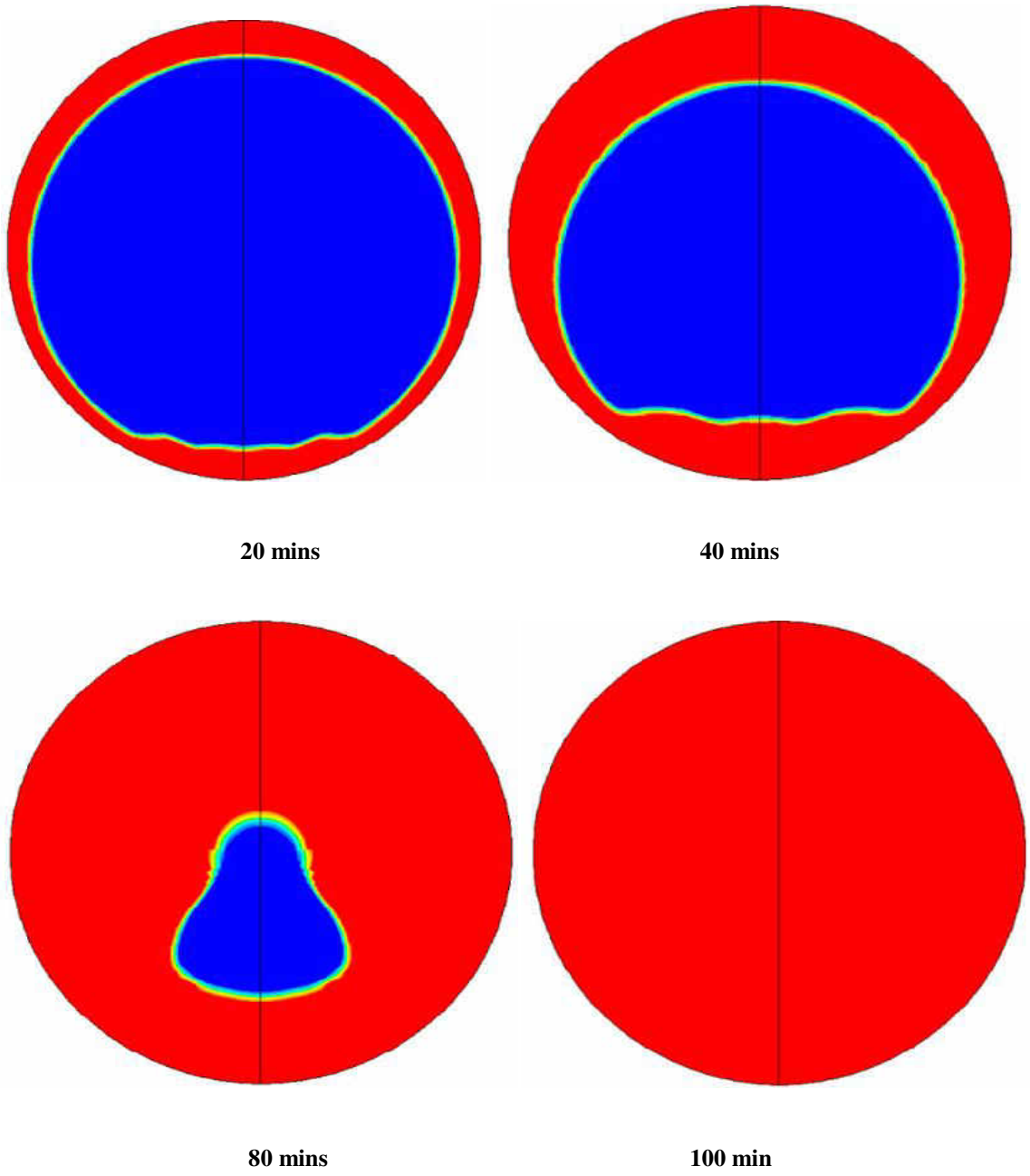

Fig. 5 – Constrained Melting Phase Front At Wall Temperature Of 40 °C And Initial Temperature Of 27.2 °C At Different Times

ISSN No: -2456 –2165

V. CFD SIMULATION OF PARAFFIN WAX PHASE CHANGE

@ 20 mins ,40 mins ,80 mins & 100 mins

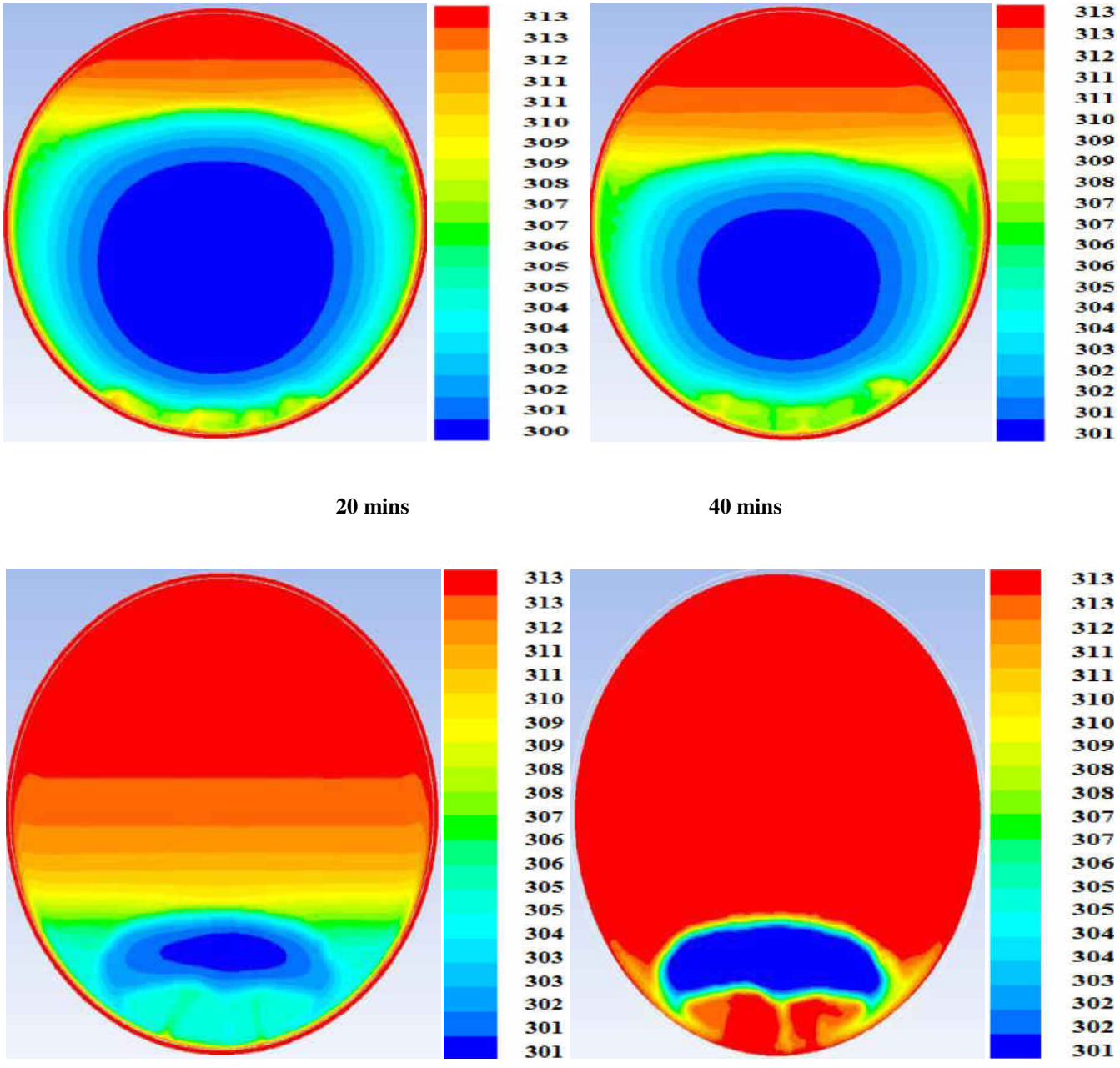

20 mins **40 mins**

60 mins **80 mins**

Fig. 6 – Detailed Temperature Contours (T in Kelvin) And Streamlines for A Wall Temperature of 40 °C at Different Time

ISSN No: -2456 –2165

VI. CFD SIMULATION OF LAURIC ACID PHASE CHANGE

@ 20 mins ,40 mins ,80 mins & 100 mins

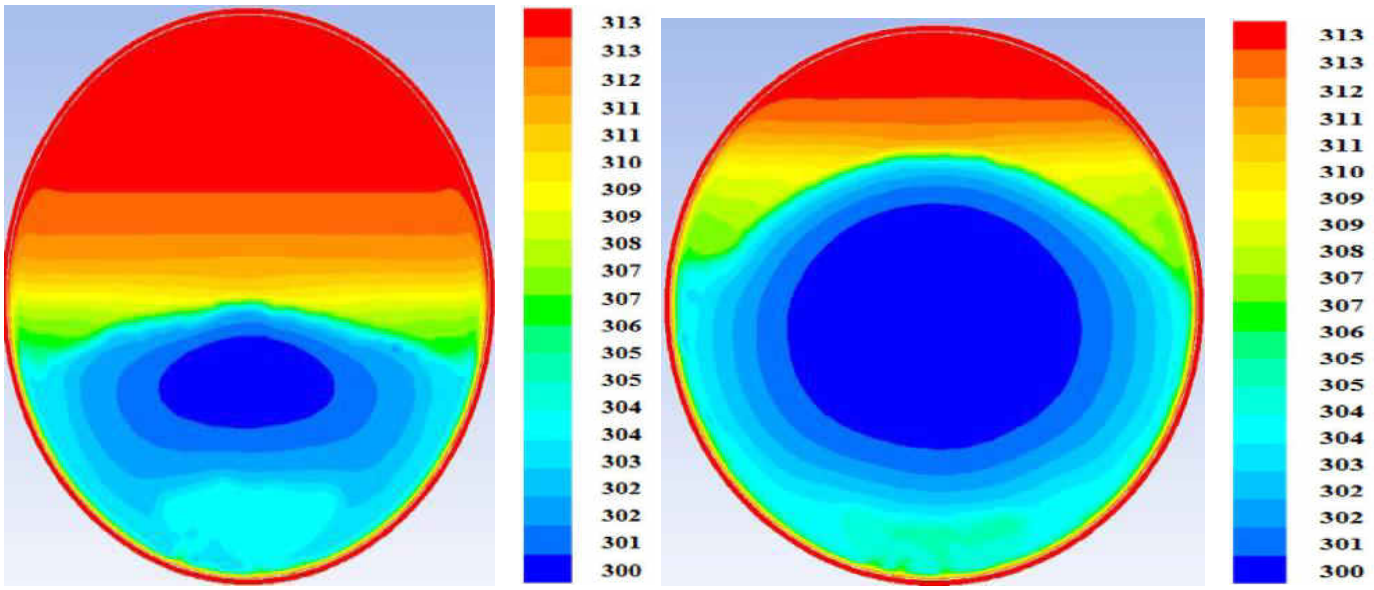

20 mins **40 mins**

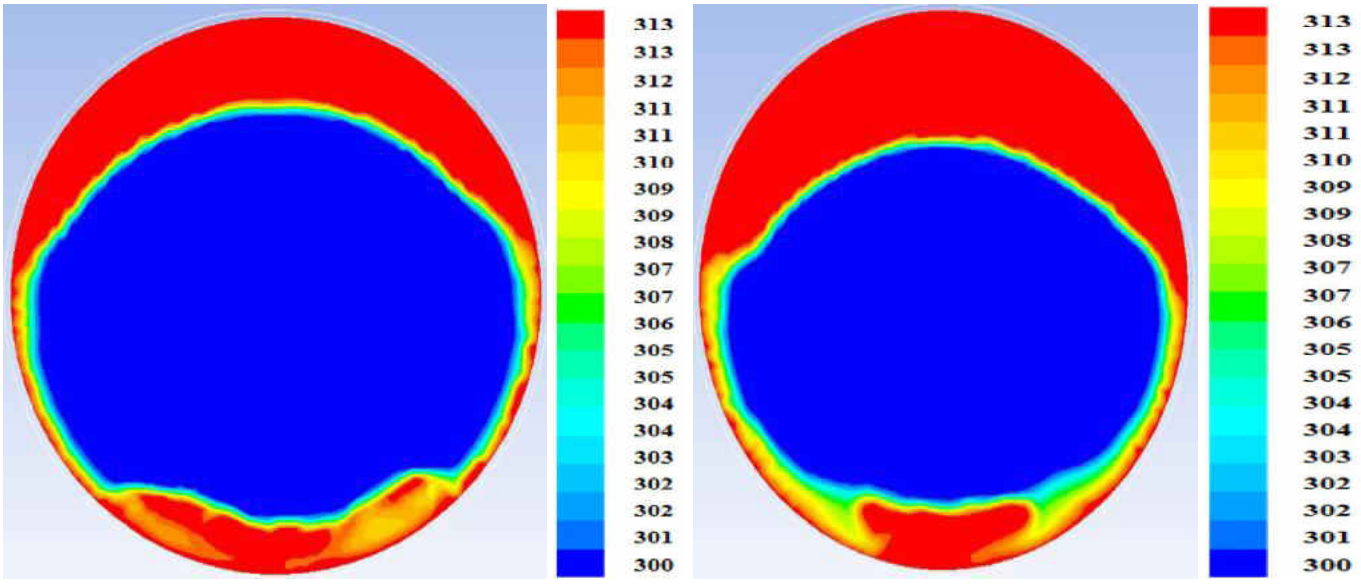

80 mins **100 mins**

ISSN No: -2456 –2165

VII. CFD SIMULATION OF SODIUM ACETATE TRI-HYDRATE PHASE CHANGE

@ 20 mins ,40 mins ,80 mins & 100 mins

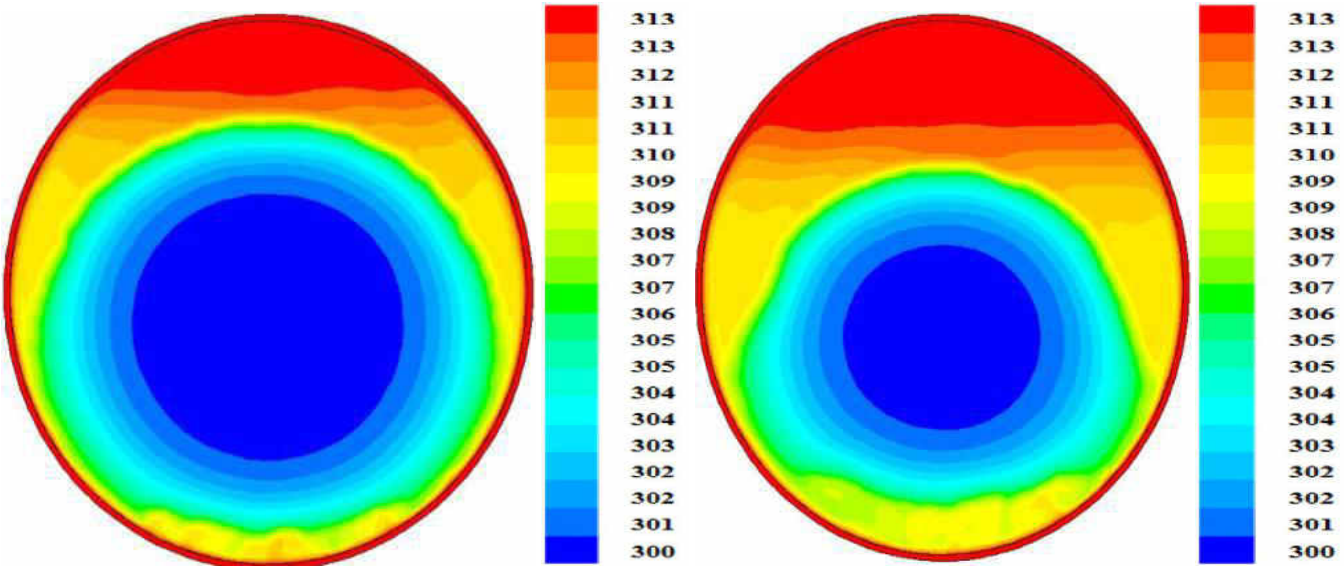

20 mins **40 mins**

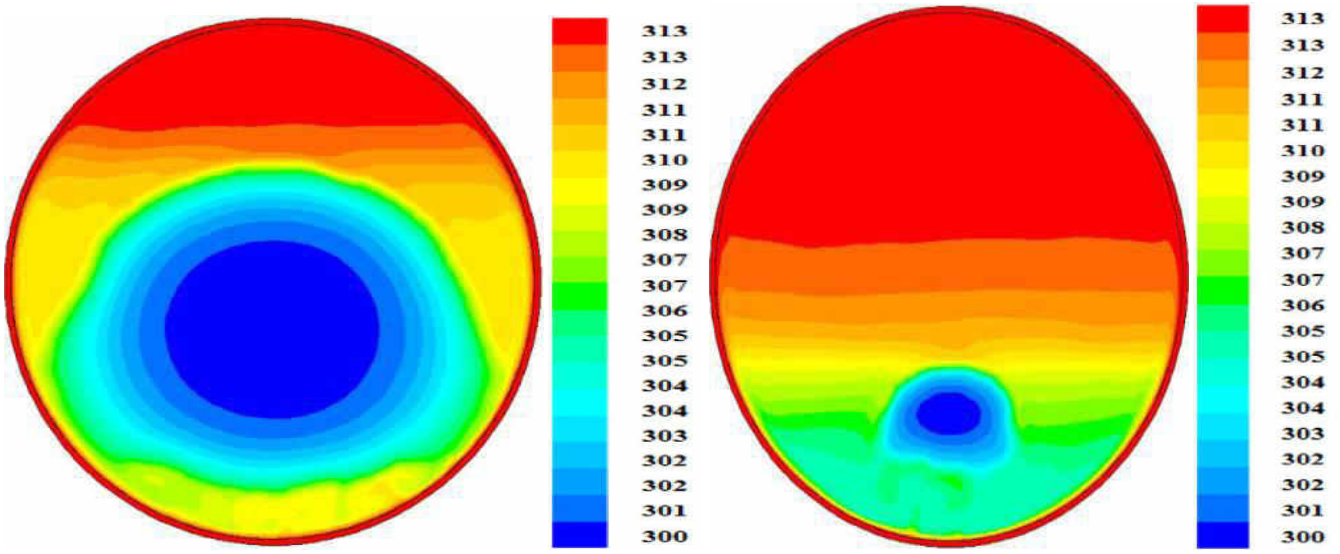

80 mins **100 mins**

ISSN No: -2456 –2165

VIII. RESULT AND DISCUSSION

A. *Comparison of Difference Materials*

The demand and supply gap for energy sources is widening day by day. Moreover, the fact that the energy can neither be created and nor destroyed has resulted in focusing of scientific research in the direction of storing the different forms of energy using diverse devices. Thermal energy is one such energy which is of interest to researchers worldwide. Thermal energy could have several geneses but storage of solar thermal energy is one of the principal areas of investigation. In recent years, various conventional and unconventional materials are investigated for their capability to store thermal energy. These thermal energy storage devices (TESD) are selected on the basis of some crucial physical, chemical and economic properties. Melting point, heat of fusion, density, heat capacity, thermal conductivity, compatibility with container and cost of production are the chief parameters for selection of TESD. It is a genuine challenge to find out an ultimate TESD as the overall suitability of materials to be used as TESD is governed by a multifaceted interplay between several properties of those Materials.

IX. CFD COMPARISON AT 40 MINS LAURIC ACID, PARAFFIN WAX AND SODIUM ACETATE TRI-HYDRATE

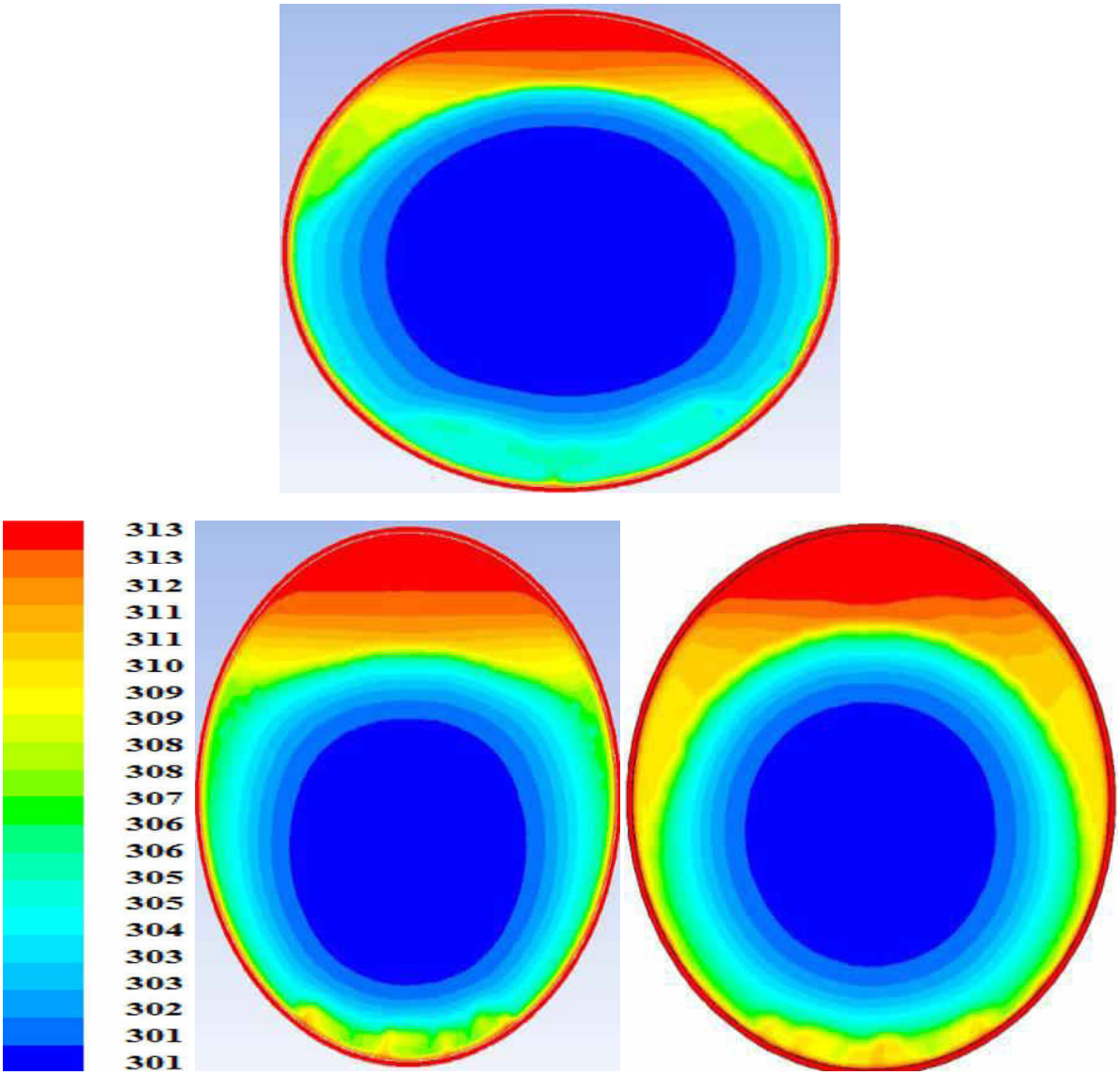

ISSN No: -2456 –2165

X. CFD COMPARISON AT 80 MINS LAURIC ACID, PARAFFIN WAX AND SODIUM ACETATE TRI-HYDRATE

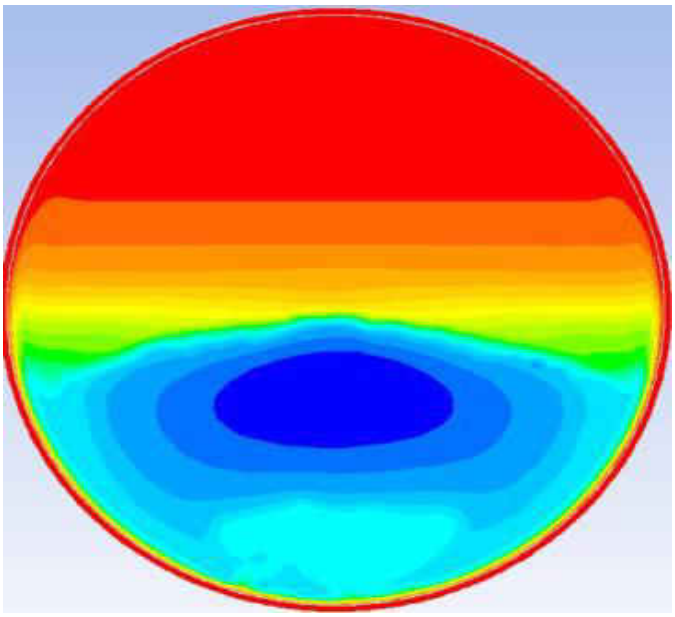

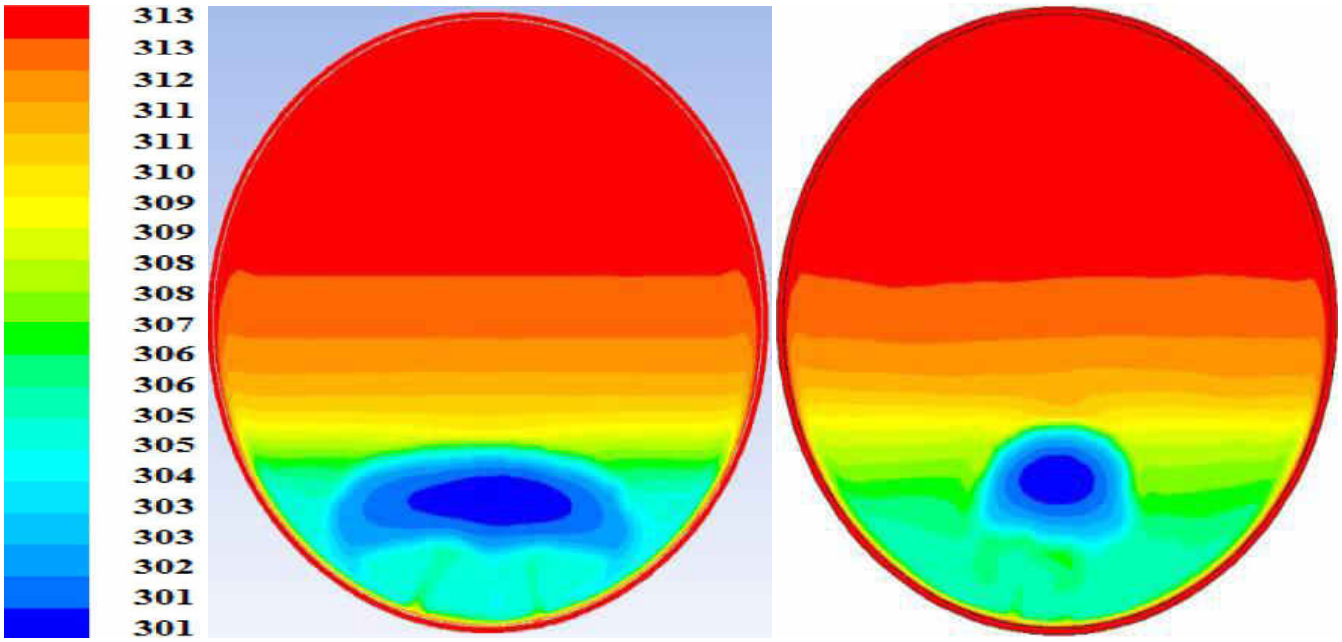

ISSN No: -2456 –2165

XI. CFD COMPARISON AT 100 MINS LAURIC ACID, PARAFFIN WAX AND SODIUM ACETATE TRI-HYDRATE

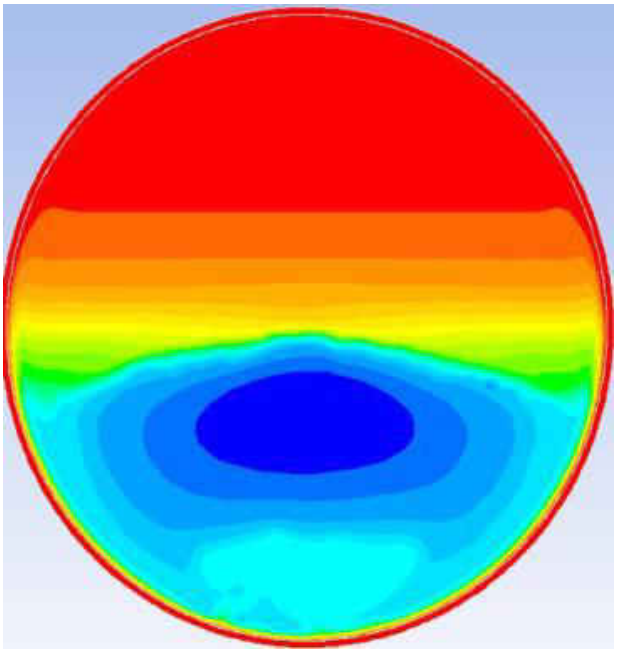

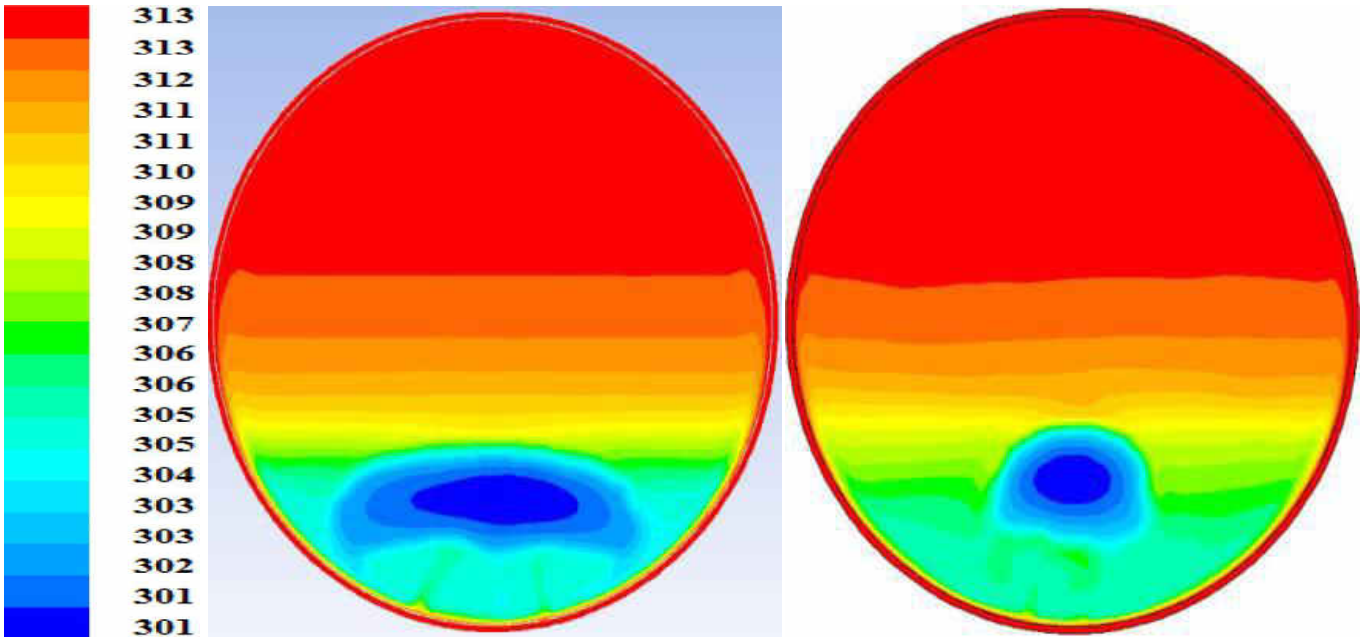

ISSN No: -2456 –2165

COMPARISON CHART

Temperature vs Time

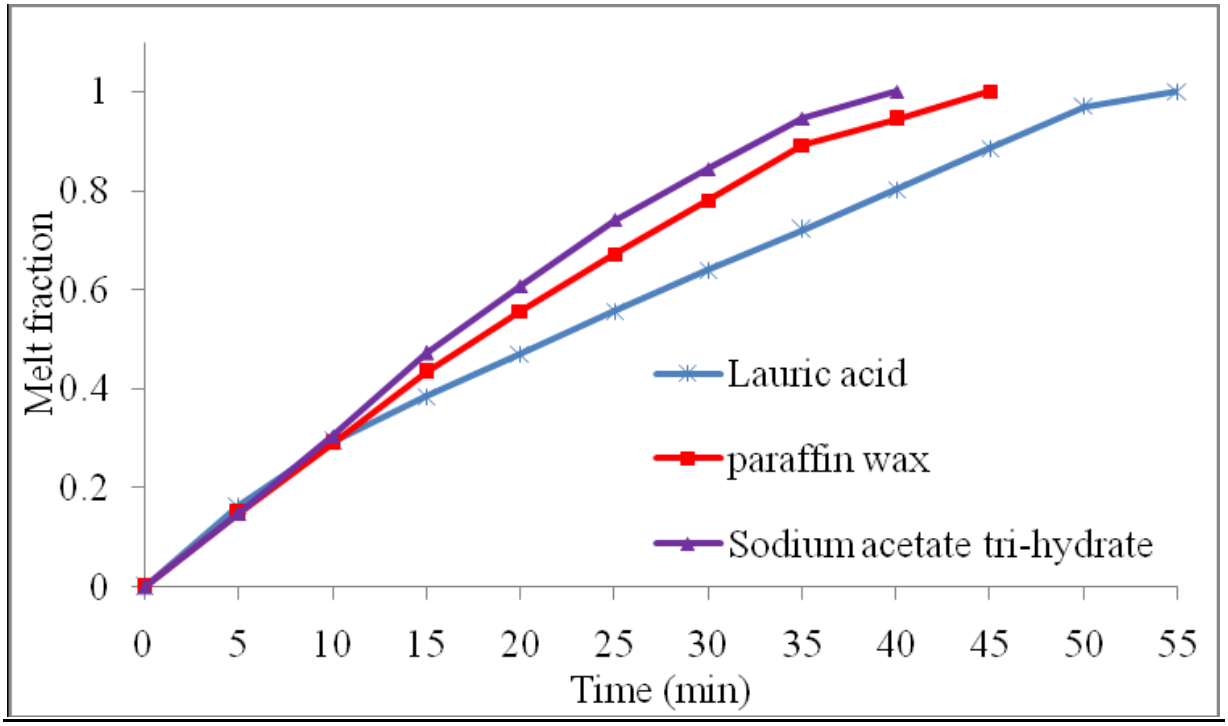

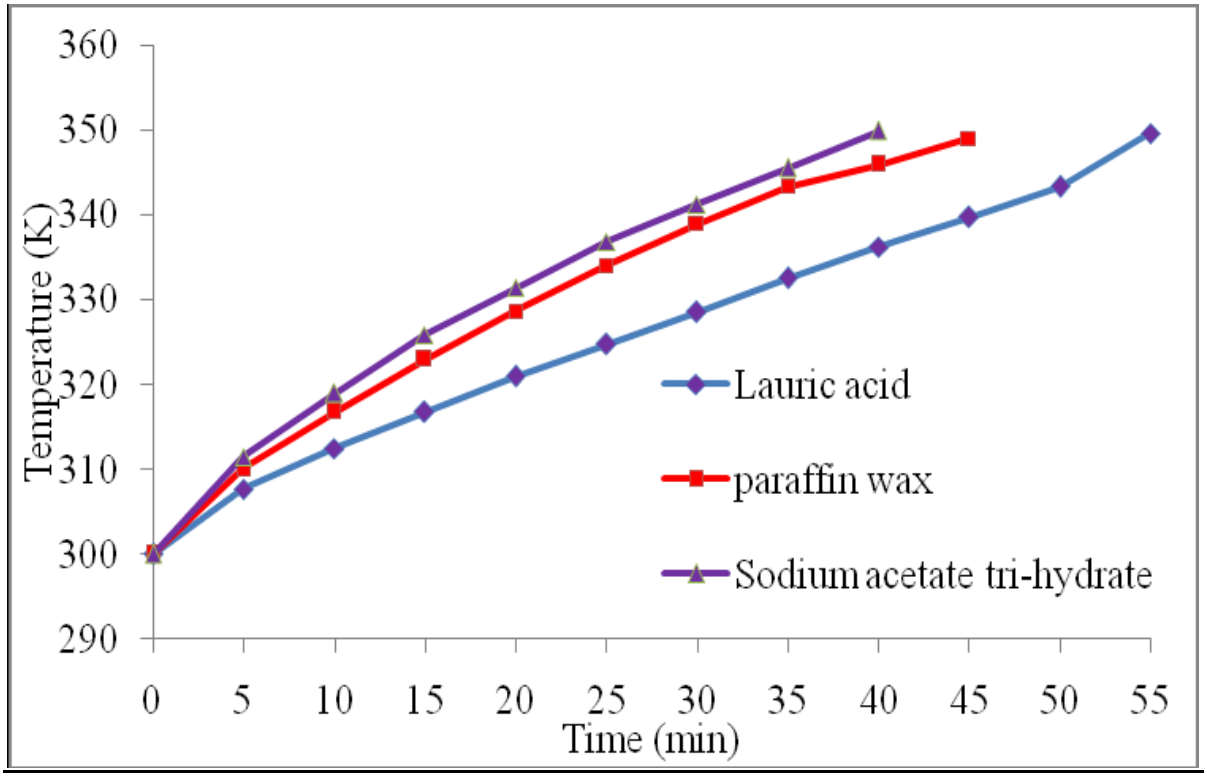

Melt Fraction vs Time

XII. CONCLUSIONS

This paper is the state of the art of phase change material. All of the PCM reviewed have a good potential for reducing cooling loads by enhancing the storage capacity. From this CFD simulation comparison, we can conclude that the SODIUM ACETATE TRI HYDRATE will have lower melt fraction than Paraffin wax and Lauric acid.

REFERENCES

[1]. Climate plan 2004: let's act together to challenge of climate change, Tech. rep., French Ministry of Ecology and Sustainable Developpment (2004).
[2]. I. Dincer, M. Rosen, Thermal Energy Storage - Systems and Applications, Jhon Wiley and Sons, 2002.
[3]. R. Baetens, B. P. Jelle, A. Gustavsen, Phase change materials for building applications: A state-of-the-art review, Energy and Buildings In Press, Accepted Manuscript (2010)
[4]. M. M. Farid, A. M. Khudhair, S. A. K. Razack, S. Al-Hallaj, A review on phase change energy storage: materials and applications, Energy Conversion and Management 45 (9-10) (2004) 1597 – 1615.
[5]. A. Pasupathy, R. Velraj, R. Seeniraj, Phase change material-based building architecture for thermal management in residential and commercial establishments, Renewable and Sustainable Energy Reviews 12 (1) (2008) 39 – 64.
[6]. A. Sharma, V. Tyagi, C. Chen, D. Buddhi, Review on thermal energy storage with phase change materials and applications, Renewable and Sustainable Energy Reviews 13 (2) (2009) 318 – 345.
[7]. U. Stritih, Heat transfer enhancement in latent heat thermal storage system for buildings, Energy and Buildings 35 (11) (2003) 1097 – 1104.
[8]. V. V. Tyagi, D. Buddhi, Pcm thermal storage in buildings: A state of art, Renewable and Sustainable Energy Reviews 11 (6) (2007) 1146 – 1166.
[9]. B. Zalba, J. M. Marn, L. F. Cabeza, H. Mehling, Free-cooling of buildings with phase change materials, International Journal of Refrigeration 27 (8) (2004) 839 – 849.
[10]. Y. Zhang, G. Zhou, K. Lin, Q. Zhang, H. Di, Application of latent heat thermal energy storage in buildings: State-of-the-art and outlook, Building and Environment 42 (6) (2007) 2197 – 2209.